

Initial Results from the CHOOZ Long Baseline Reactor Neutrino Oscillation Experiment

M. Apollonio^c, A. Baldini^b, C. Bemporad^b, E. Caffau^c, F. Ci^b, Y. Déclais^e,
H. de Kerret^f, B. Dieterle^h, A. Etenko^d, J. George^h, G. Giannini^c, M. Grassi^b,
Y. Kozlov^d, W. Kropp^g, D. Krynf^f, M. Laiman^e, C.E. Lane^a, B. Lefièvre^f,
I. Machulin^d, A. Martemyanov^d, V. Martemyanov^d, L. Mikaelyan^d, D. Nicolò^b,
M. Obolensky^f, R. Pazzi^b, G. Pieri^b, L. Price^g, S. Riley^g, R. Reeder^h,
A. Sabelnikov^d, G. Santin^c, M. Skorokhvatov^d, H. Sobel^g, J. Steele^a, R. Steinberg^a,
S. Sukhotin^d, S. Tomshaw^a, D. Veron^f, and V. Vyrodov^f

^a*Drexel University*

^b*INFN and University of Pisa*

^c*INFN and University of Trieste*

^d*Kurchatov Institute*

^e*LAPP-IN2P3-CNRS Annecy*

^f*PCC-IN2P3-CNRS Collège de France*

^g*University of California, Irvine*

^h*University of New Mexico, Albuquerque*

PACS: 14.16.P, 28.50.Hw

Abstract

Initial results are presented from CHOOZ¹, a long-baseline reactor-neutrino vacuum-oscillation experiment. The data reported here were taken during the period March to October 1997, when the two reactors ran at combined power levels varying from zero to values approaching their full rated power of 8.5 GW (thermal). Electron antineutrinos from the reactors were detected by a liquid scintillation calorimeter located at a distance of about 1 km. The detector was constructed in a tunnel protected from cosmic rays by a 300 MWE rock overburden. This massive shielding strongly reduced potentially troublesome backgrounds due to cosmic-ray muons, leading to a background rate of about one event per day, more than an order of magnitude smaller than the observed neutrino signal. From the statistical agreement between detected and expected neutrino event rates, we find (at 90% confidence level) no evidence for neutrino oscillations in the $\bar{\nu}_e$ disappearance mode for the parameter region given approximately by $\Delta m^2 > 0.9 \cdot 10^{-3} \text{ eV}^2$ for maximum mixing and $\sin^2 2\theta > 0.18$ for large Δm^2 .

Key words: reactor, neutrino mass, neutrino mixing, neutrino oscillations

¹ The CHOOZ experiment is named after the new nuclear power station operated by Électricité de France (EdF) near the village of Chooz in the Ardennes region of France.

1 Introduction

In the widely accepted Standard Model of electroweak interactions, neutrinos have zero rest mass. Since neutrino oscillation experiments sensitively probe the existence of finite neutrino mass, such experiments are important for testing and possibly improving the Standard Model. These experiments are especially intriguing at present because they yield a number of hints of significant neutrino oscillation effects [1]. If validated, these hints imply that changes in the Standard Model are required. Furthermore, a finite neutrino mass could have significant consequences in many aspects of astrophysics and cosmology.

The neutrino oscillation experiments measure neutrino fluxes from greatly differing sources. Each of a number of experiments measuring solar neutrino fluxes on earth always finds values smaller than the expected ones. Various interpretations of these results in terms of an oscillation-induced disappearance of electron neutrinos have been offered.

Several atmospheric (“cosmic-ray”) neutrino experiments find ν_μ/ν_e ratios that are anomalously low by about a factor of two, indicating a disappearance of ν_μ or possibly an appearance of ν_e .

These experimental results are often presented in the context of a model with two neutrino eigenstates of mass m_1 and m_2 which mix to form two flavour states. A pure beam of electron-flavoured neutrinos has a survival probability which oscillates due to the $m_1 - m_2$ mass difference. For a single neutrino energy $E_\nu(\text{MeV})$ and a distance from the source L (meters), the survival probability can be written in terms of the mixing parameter $\sin^2 2\theta$ and the difference of the squared masses $\Delta m^2 = |m_2^2 - m_1^2|$ as follows:

$$P(\bar{\nu}_e \rightarrow \bar{\nu}_e) = 1 - \sin^2 2\theta \sin^2 \left(\frac{1.27 \Delta m^2 (\text{eV}^2) L (\text{m})}{E_\nu (\text{MeV})} \right).$$

When averaged over the source energy spectrum, this formula links the disappearance of neutrinos to neutrino mass.

Due to their large values of L/E , the solar neutrino experiments favour Δm^2 values in the range 10^{-5} to 10^{-10} eV^2 , while the cosmic-ray neutrino results give 10^{-1} to 10^{-3} eV^2 . Ambiguities persist in the interpretation of the cosmic-ray neutrino ratio; the ν_μ flux may be low due to either oscillation of $\nu_\mu \leftrightarrow \nu_\tau$ or to $\nu_\mu \leftrightarrow \nu_e$.

The CHOOZ experiment [2] has an average value of $L/E \sim 300$ ($L \sim 1$ km, $E \sim 3$ MeV), an intense and nearly pure neutrino flavour composition ($\sim 100\%$ $\bar{\nu}_e$) and an intensity known to better than 2%. It is thus ideally suited for a definitive test of $\bar{\nu}_e \rightarrow \bar{\nu}_\mu$ neutrino oscillations (or, more generally, $\bar{\nu}_e \rightarrow \bar{\nu}_x$ oscillations) down to 10^{-3} eV^2 , an order of magnitude lower than previous reactor experiments [3-7]. CHOOZ focuses directly on the cause of the cosmic-ray anomaly and greatly increases the mass range explored by neutrino experiments having well understood flux and composition.

2 Description of the CHOOZ Experiment

2.1 The Neutrino Source

The Chooz power station has two pressurized water reactors with a total thermal power of 8.5 GW_{th}. The first reactor reached full power in May 1997, the second in August 1997. The $\bar{\nu}_e$ flux and energy spectrum of similar reactors have been extensively studied. Analogous methods [3,8] have been used to calculate the $\bar{\nu}_e$ flux emitted by the Chooz reactors. The calculation includes

- a full description of the reactor core including the initial ^{235}U enrichment and the daily evolution [9] of the isotopic composition of each fuel element as a function of the power produced (burn-up),
- the instantaneous fission rate derived from the thermal power of the reactors (recorded every minute),
- the $\bar{\nu}_e$ yield (as determined in [10–12]) from the four main isotopes – ^{235}U , ^{238}U , ^{239}Pu , and ^{241}Pu .

It has been shown [3] that the value of the $\bar{\nu}_e$ flux emitted by a reactor is understood to 1.4%. For this reason there is no need for a normalization experiment to measure the $\bar{\nu}_e$ flux with a detector close to the reactors.

2.2 The Site

The detector is located in an underground laboratory at a distance of about 1 km from the neutrino source. The 300 MWE rock overburden reduces the external cosmic ray muon flux by a factor of ~ 300 to a value of $0.4 \text{ m}^{-2}\text{s}^{-1}$, significantly decreasing the most dangerous background, which is caused by fast neutrons produced by muon-induced nuclear spallation in the materials surrounding the detector. This cosmic ray shielding is an important feature of the CHOOZ site.

The detector (Fig. 1) is installed in a welded cylindrical steel vessel 5.5 m in diameter and 5.5 m deep. The inside walls of the vessel are painted with high-reflectivity white paint. The vessel is placed in a pit 7 m in diameter and 7 m deep. To protect the detector from the natural radioactivity of the rock, the steel vessel is surrounded by 75 cm of low radioactivity sand (Comblanchien from Burgundy in France) and covered by 14 cm of cast iron.

2.3 The Detector

The $\bar{\nu}_e$ are detected via the inverse beta decay reaction

$$\bar{\nu}_e + p \rightarrow e^+ + n \quad \text{with} \quad E_{e^+} = E_{\bar{\nu}_e} - 1.804 \text{ MeV} .$$

The $\bar{\nu}_e$ signature is a delayed coincidence between the prompt e^+ signal (boosted by the two 511-keV annihilation gamma rays) and the signal from the neutron capture. The target material is a hydrogen-rich (free protons) paraffinic liquid scintillator loaded with 0.09% gadolinium. The target is contained in an acrylic

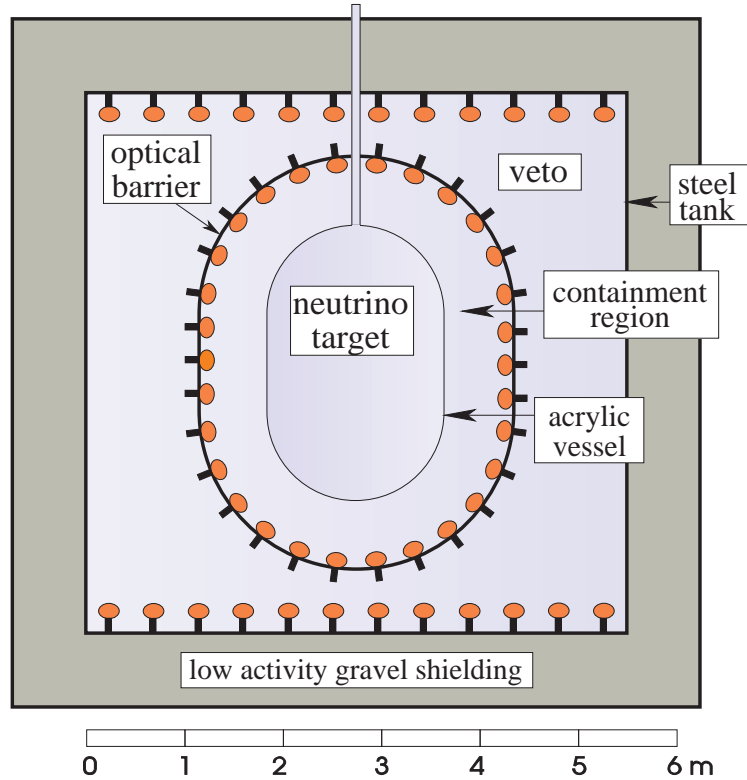


Figure 1: The CHOOZ detector.

vessel of precisely known volume immersed in a low energy calorimeter made of unloaded liquid scintillator. Gd has been chosen due to its large neutron capture cross section and to the high γ -ray energy released after n-capture (~ 8 MeV, well above the natural radioactivity).

The detector is made of three concentric regions:

- a central 5-ton target in a transparent plexiglass container filled with a 0.09% Gd-loaded scintillator (“region 1”);
- an intermediate 17-ton region (70 cm thick) equipped with 192 eight-inch PMT’s (15% surface coverage, ~ 130 photoelectrons/MeV) [13], used to protect the target from PMT radioactivity and to contain the gamma rays from neutron capture (“region 2”);
- an outer 90-ton optically separated active cosmic-ray muon veto shield (80 cm thick) equipped with two rings of 24 eight-inch PMT’s (“region 3”).

The detector is simple and easily calibrated, while its behaviour can be well checked. Six laser flashers are installed in the three regions together with calibration

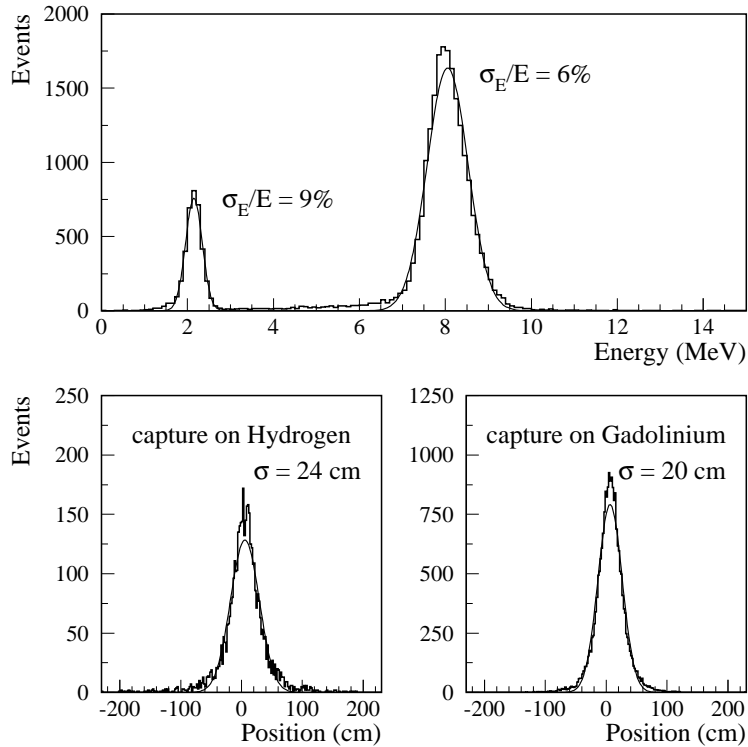


Figure 2: Energy and position resolution for ^{252}Cf n -capture γ -lines.

pipes to allow the introduction of radioactive sources. The detector can be reliably simulated by the Montecarlo method [14].

The first target filling needed to be replaced after about four months of operation due to a problem with the Gd-loaded scintillator — reduced transparency of the scintillator caused by a chemical instability. After protecting with teflon all metallic parts in contact with the liquid and after slightly modifying the scintillator formula for improved stability, we now operate with a new filling introduced in March 1997. The new scintillator has a measured useful lifetime in the detector (due to reduced light at the PMT's) of $\tau \sim 750$ d.

The period with the first scintillator fill was very useful in tuning the detector and in establishing the appropriate calibration methods and analysis procedures. All data used in the present paper were gathered using the second batch of scintillator.

Fig. 2 shows calibration data using a ^{252}Cf source at the detector centre. The neutron capture lines (2.2 MeV on hydrogen and 8 MeV on gadolinium) are clean and the energy resolutions are $\sigma_E/E = 9\%$ and $\sigma_E/E = 6\%$, respectively.

2.4 Trigger and Acquisition Electronics

The experiment is triggered using a two-level, two-threshold scheme. Level-one triggers, formed by discriminating the total PMT charge and hit multiplicity, correspond to deposited energies of 1.3 MeV ($L1_{low}$, rate $\sim 130\text{ s}^{-1}$) and 3.3 MeV ($L1_{high}$, rate $\sim 30\text{ s}^{-1}$). The level-two trigger (L2) requires a delayed coincidence of $L1_{low}$ and $L1_{high}$ within $100\ \mu\text{s}$. Both pulse sequences are allowed in order to permit study of the accidental background. Finally, the readout of neutrino candidate events (rate $\sim 0.15\text{ s}^{-1}$) is triggered by an L2 preceded by at least a 1 ms time interval with no activity in the veto shield.

The data acquisition system consists of several redundant digitization systems controlled by a VME-based processor. Each PMT signal is digitized by a multi-hit TDC and by one of two alternating ADC banks, gated by $L1_{low}$. Signals from groups of 8 PMT's, referred to as *patches*, are fanned-in and recorded by fast (150 MHz, $8 \times 206\text{ ns}$ deep) and slow (20 MHz, $200\ \mu\text{s}$ deep) waveform digitizers and by two banks of multi-hit VME ADC's gated by $L1_{low}$. The latter provide charge information for a total of nine $L1_{low}$ events. The VME ADC's are also connected with a neural-network-based event reconstruction fast processor (NNP) [15]. The NNP reconstructs the position and the energy of events in $\sim 150\ \mu\text{s}$, allowing study of events corresponding to much lower energy thresholds than those permitted by the main CHOOZ trigger.

3 Data Analysis

3.1 Event Selection and Reconstruction

The redundancy in the digitization electronics allows a good check of data quality. It has been found that using the 8:1 fanned-in patches results in good energy and position resolutions. The results presented in this paper are based on the 8:1 fanned-in VME ADC data, fitted by a MINUIT-based procedure to obtain energy and position. Procedures using other charge and time information are also being studied.

The selection of events is based on the following requirements:

- energy cuts on the neutron candidate (6 – 12 MeV) and on the e^+ (from the $L1_{low}$ threshold energy to 8 MeV),
- a time cut on the delay between the e^+ and the neutron ($2 - 100\ \mu\text{s}$),
- spatial cuts on the e^+ and the neutron (distance from the PMT wall $> 30\text{ cm}$ and distance $n - e^+ < 100\text{ cm}$).

The events are then divided in two classes. The first class contains the neutrino candidates, in which the e^+ precedes the n , while the second consists of events in which the n precedes the e^+ . The second class of events is used to establish the rate of accidentals and of multiple neutron events. These events provide a good test of the stability of the background throughout the data taking periods.

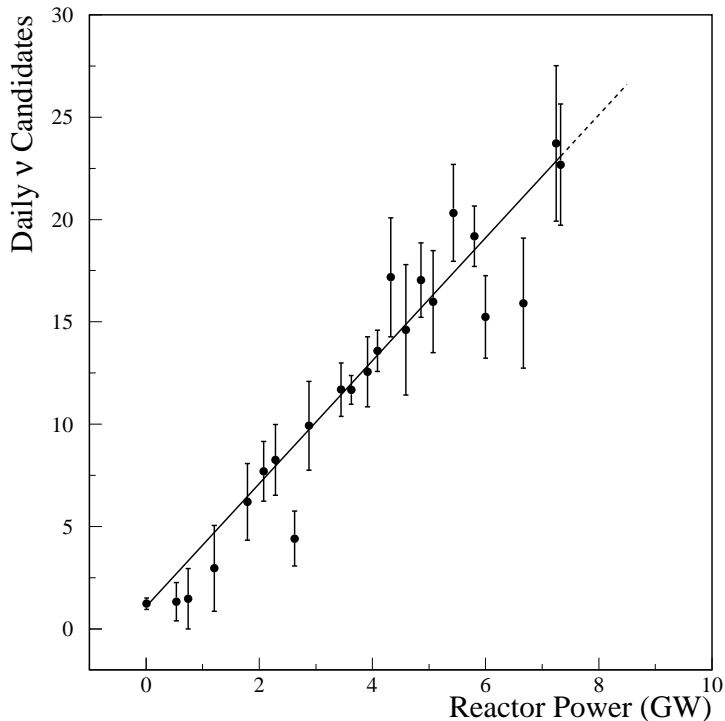


Figure 3: Number of $\bar{\nu}_e$ -candidates d^{-1} , as a function of the reactor power.

3.2 Background and Neutrino Signal

The neutrino signal was obtained by subtracting the small number of accidental and correlated background events which passed the neutrino selection criteria. These two components were determined separately. The accidental component was estimated by using the e^+ and n uncorrelated rates. The correlated component was estimated from reactor-off data by extrapolating the rate of high-energy neutrons followed by n -capture into the region defined by the ν event selection criteria. The background rates were found to be

$$R_{\text{accidental}} = 0.23 \pm 0.05 \text{ d}^{-1} \text{ and } R_{\text{correlated}} = 0.8 \pm 0.2 \text{ d}^{-1}.$$

The total background rate was measured with reactor-off and also by extrapolating the neutrino candidate rate to zero reactor power. For this purpose, neutrino candidates were collected during the period of reactor power rise. The number of events corresponding to each data run depended on the run duration ΔT and on the average reactor power W_{av} . All data were therefore fitted as a function of these two variables, thus separately determining the neutrino signal and the reactor-off background. The (grouped) data are shown in Fig. 3 as a function of reactor power. The superimposed line corresponds to the fitted signal and background values. The results of the various background determinations are summarized in Table 1.

Table 1. Background Rates

| | |
|-------------------------------------|--------------------------------|
| estimated rate | $1.03 \pm 0.21 \text{ d}^{-1}$ |
| reactor-off rate | $1.2 \pm 0.3 \text{ d}^{-1}$ |
| rate by extrapolation to zero power | $1.1 \pm 0.25 \text{ d}^{-1}$ |

It should be noted that the measurements of the background are in good agreement. From the fit we find the neutrino rate S_{fit} normalized to the full power of the two reactors ($2 \times 4.25 \text{ GW}_{th}$, $2 \times 1.3 \times 10^{20}$ fissions s^{-1}) and a burn-up of $1300 \text{ MW d ton}^{-1}$ to be

$$S_{fit} = 25.5 \pm 1.0 \text{ d}^{-1}.$$

A total of 1320 neutrino events were accumulated during 2718 hours (live time). The distribution of their physical parameters (neutron capture energy and time, $n - e^+$ distance) is presented in Fig. 4; a neutron delay distribution obtained by a ^{252}Cf source is also shown. Using the total number of events and subtracting the reactor-off background, we obtain the similar, but slightly less accurate, result

$$S_{integral} = 25.0 \pm 1.1 \text{ d}^{-1}.$$

4 Expected Number of Events and Systematic Errors

The expected number of detected neutrino events can be written

$$N_{ev} = N_{fiss} \times \sigma_{fiss} \times \frac{1}{4\pi D^2} \times n_p \times \epsilon_{e^+} \times \epsilon_n \times \epsilon_{\Delta r} \times T_{live} ,$$

where

- N_{fiss} is the number of fissions, per unit time, in the reactor cores,
- σ_{fiss} is the cross section [4,16,17] for the reaction $\bar{\nu}_e + p \rightarrow e^+ + n$ calculated for a neutron lifetime of $887.0 \pm 2.0 \text{ s}$ [18], and integrated over the $\bar{\nu}_e$ energy spectrum and the fuel composition of the core,
- D is the distance of the detector from the reactors,
- n_p is the effective number of free protons in the target, including small corrections for edge effects involving the acrylic vessel and the region 2 scintillator buffer,
- ϵ_{e^+} and ϵ_n are the positron and neutron detection efficiencies averaged over the entire sensitive target,
- $\epsilon_{\Delta r}$ is the efficiency of the $e^+ - n$ distance cut, and
- T_{live} is the live time.

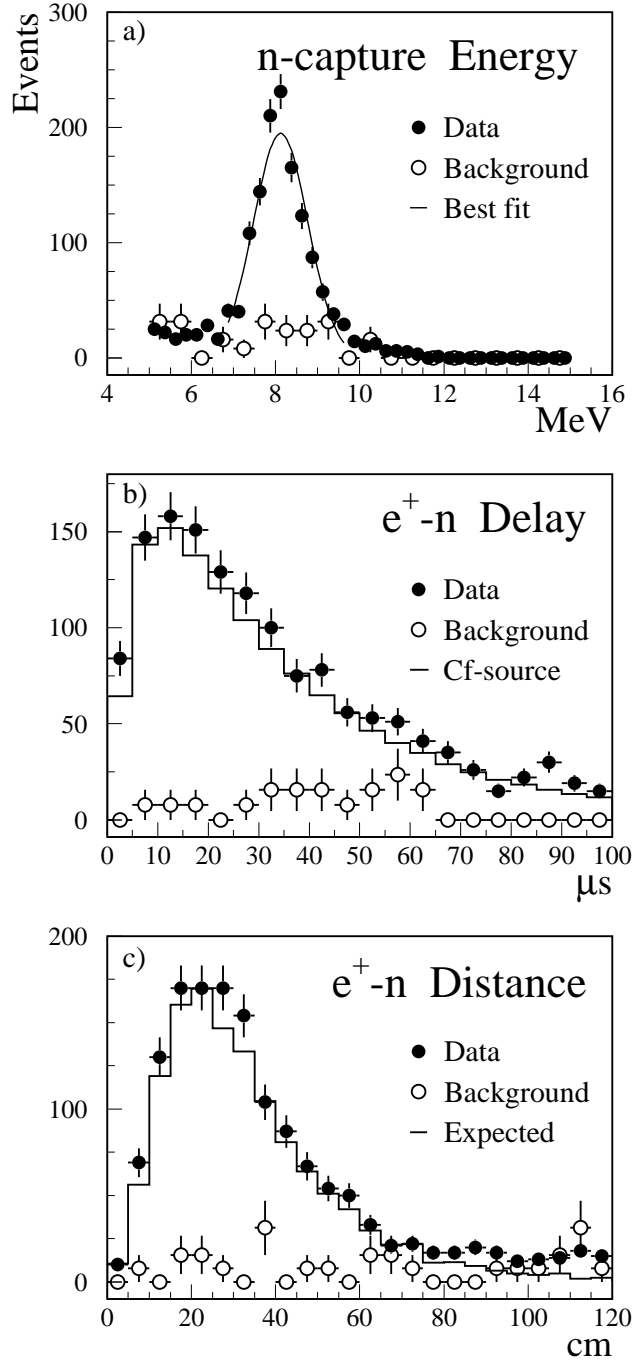


Figure 4: Distribution of: a) energy released by n -capture on Gd, b) n -capture delay, c) positron-neutron distance, measured and MC expected; the reactor-off background distribution is also shown. The histograms in b) and c) are normalized to the background subtracted experimental data.

Table 2 shows the various parameters together with their errors. The combined systematic error is estimated at $\sim 4\%$.

Table 2. Normalization Parameters and Errors

| Parameter | Value | Error |
|---|--------------------------------------|-------|
| cross section per fission | $6.327 \times 10^{-43} \text{ cm}^2$ | 2.7% |
| reactor 1 distance | $1.1146 \times 10^5 \text{ cm}$ | 10 cm |
| reactor 2 distance | $0.9979 \times 10^5 \text{ cm}$ | 10 cm |
| number of free protons in the Gd-loaded scintillator | 3.601×10^{29} | 1.5% |
| effective number of free protons in the target | 3.637×10^{29} | 1.5% |
| e^+ efficiency | 0.968 | 0.7% |
| measured n efficiency at centre (^{252}Cf data) | 0.757 | 1.3% |
| calculated n efficiency at centre (Monte Carlo) | 0.759 | 1.3% |
| n efficiency averaged over the effective volume | 0.739 | 2.0% |
| efficiency of the $e^+ - n$ distance cut | 0.965 | 1.4% |

5 Results

The ratio of the measured to expected neutrino signal is

$$R_{\text{measured/expected}} = 0.98 \pm 0.04(\text{stat}) \pm 0.04(\text{syst}).$$

One can also compare the measured positron spectrum with what is expected in the case of no oscillations (Fig. 5). The 90% C.L.exclusion plot is presented in Fig. 6, together with the exclusion plots of previous experiments and the atmospheric neutrino signal reported by Kamiokande [19].

6 Conclusions

The CHOOZ experiment finds, at 90% C.L., no evidence for neutrino oscillations in the disappearance mode $\bar{\nu}_e \rightarrow \bar{\nu}_x$ for the parameter region given approximately by $\Delta m^2 > 0.9 \cdot 10^{-3} \text{ eV}^2$ for maximum mixing and $\sin^2 2\theta > 0.18$ for large Δm^2 , as shown in Fig. 6.

The experiment is continuing to take data in order to achieve better statistics and to improve understanding of systematic effects.

7 Acknowledgements

Construction of the laboratory was funded by Électricité de France (EdF). Other work was supported in part by IN2P3-CNRS (France), INFN (Italy), the United States Department of Energy, and by RFBR (Russia). We are very grateful to

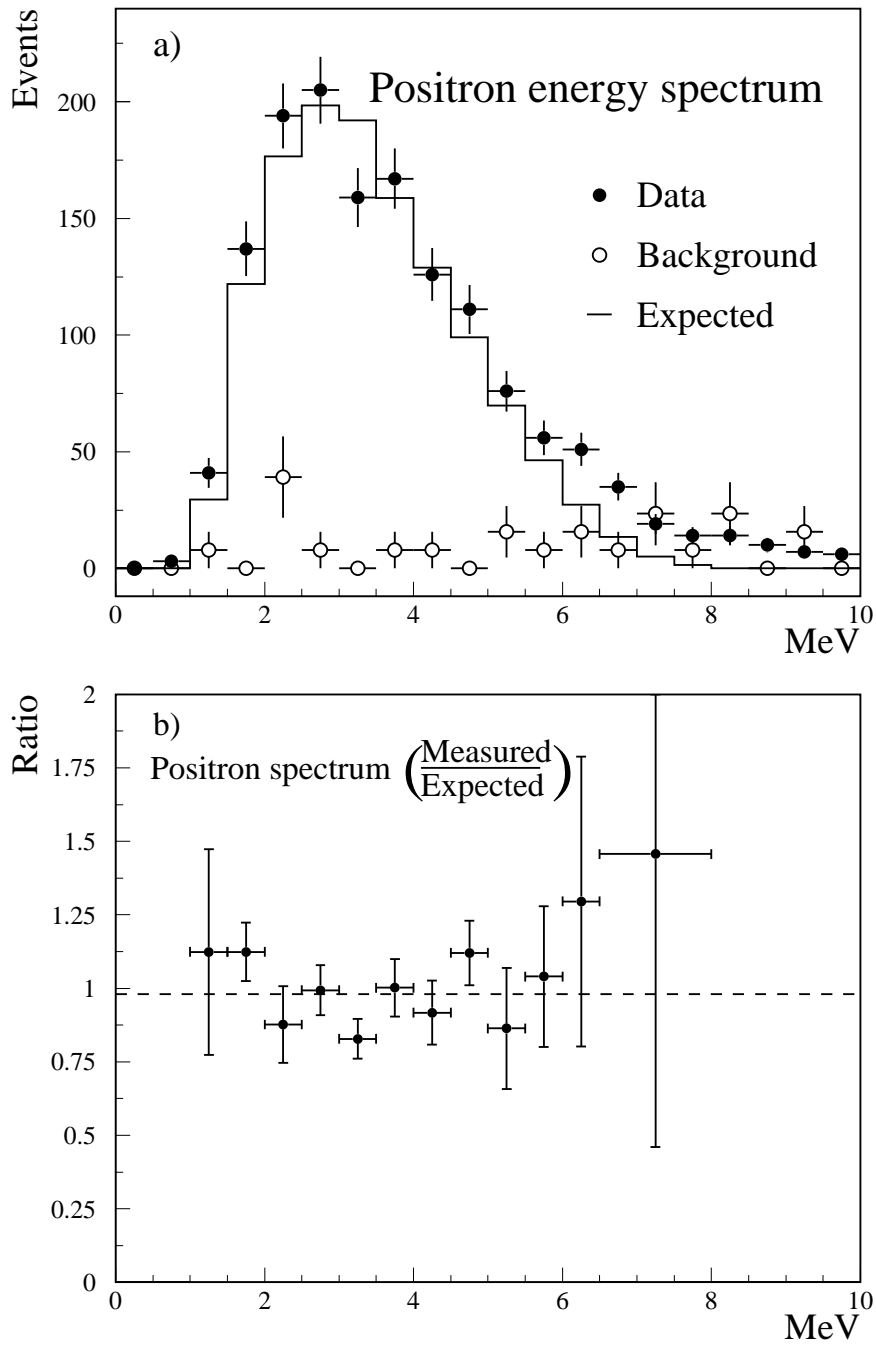


Figure 5: a) Positron energy spectrum and corresponding reactor-off background for the same live-time; the neutrino-signal expected positron spectrum is also shown. b) Ratio of the measured (background subtracted) to the expected positron spectrum.

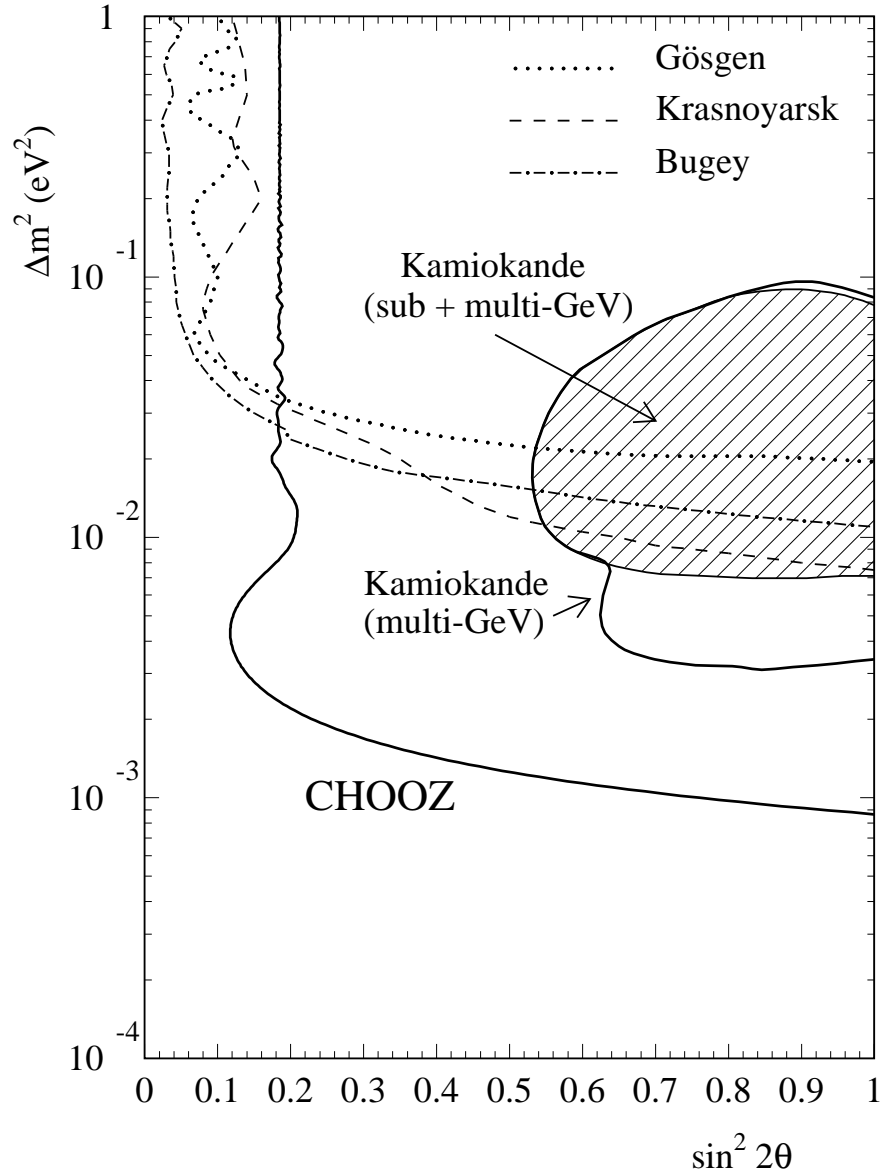


Figure 6: The 90% C.L. exclusion plot for CHOOZ, compared with previous experimental limits and with the KAMIOKANDE allowed region.

the Conseil Général des Ardennes for having provided us with the headquarters building for the experiment. At various stages during construction and running of the experiment, we benefited from the efficient work of personnel from SENA (Société Electronucléaire des Ardennes) and from the EdF Chooz B nuclear plant. Special thanks to the technical staff of our laboratories for their excellent work in designing and building the detector.

References

- [1] For a review see M. Nakahata, Neutrino Masses and Oscillations, summary talk, HEP97, Jerusalem (1997).
- [2] The CHOOZ Collaboration, Proposal. Available on the internet at http://duphy4.physics.drexel.edu/chooz_pub/ .
- [3] Y. Declais *et al.*, Phys. Lett. B**338** (1994) 383.
- [4] B. Achkar *et al.*, Nucl. Phys. B**434** (1995) 503.
- [5] G.S. Vidyakin *et al.*, JETP Lett. **59** (1994) 364.
- [6] G. Zacek *et al.*, Phys. Rev. D**34** (1986) 2621.
- [7] Z.D. Greenwood *et al.*, Phys. Rev. D**53** (1996) 6054.
- [8] B. Achkar *et al.*, Phys. Lett. B**374** (1996) 243.
- [9] E. Martino, Électricité de France–SEPTEN, Lyon.
- [10] K. Schreckenbach *et al.*, Phys. Lett. B**160** (1985) 325.
- [11] P. Vogel, Phys. Rev. C**24** (1981) 1543.
- [12] A.A. Hahn *et al.*, Phys. Lett. B**218** (1989) 365.
- [13] A. Baldini *et al.*, Nucl. Instrum. Methods A**372** (1996) 207.
- [14] H. de Kerret, B. Lefièvre, Simulation des Neutrons de Basse Energie, LPC–Collège de France, LPC 88–01.
- [15] A. Baldini *et al.*, Nucl. Instrum. Methods A**389** (1997) 1441.
- [16] P. Vogel, Phys. Rev. D**29** (1984) 1918.
- [17] V. Kopeikin *et al.*, Kurchatov note IAE–6026/2, Moscow 1997.
- [18] Particle Data Group, Phys. Rev. D**54** (1996) 1.
- [19] Y. Fukuda *et al.*, Phys. Lett. B**335** (1994) 237.